Collision Detection in IEEE 802.11 Networks by Error Vector Magnitude Analysis

Muhammad Naveed Aman†, Wai Kin Chan‡, and Biplab Sikdar†
†Department of ECSE, ‡Department of ISE
Rensselaer Polytechnic Institute, Troy, NY 12180 USA

***Abstract*—There are two causes of packet losses during a wireless transmission: losses caused by collisions and losses caused by poor channel conditions. The throughput and spatial reuse of IEEE 802.11 based wireless networks, as well as the effectiveness of the rate adaptation algorithms they use, is adversely affected by their inability to determine the real cause of a packet loss. To address this issue, this paper proposes a mechanism based on Error Vector Magnitude (EVM) to discern random channel errors from collisions in wireless networks. The proposed mechanism is based on first developing an analytic model to characterize the EVM of a packet in the presence and absence of a collision. A threshold based classifier is then proposed that selects the threshold value such that the crossover error rate is achieved. Simulation results are presented to demonstrate the accuracy of the proposed collision detection mechanism.**

I. Introduction

Wired networks like Ethernet (IEEE 802.3) use carrier sense multiple access with collision detection (CSMA/CD) as the basis for medium access control. A wired network can detect collisions because of its ability to listen at the same time it transmits. The wireless environment brings with it different challenges, one of them being the difficulty to transmit and receive at the same time. Moreover, while a node in a wired network can receive every other node's transmissions, a node on a wireless network may be too far (or hidden) from certain other nodes to receive their transmissions (and vice versa) [6]. Thus, wireless networks like IEEE 802.11 use a mechanism called carrier sense multiple access with collision avoidance (CSMA/CA) at the MAC layer.

The physical layer of IEEE 802.11 delivers a packet to the MAC layer only if it has been received correctly, otherwise the packet is discarded. A fundamental issue with the use of CSMA/CA based protocols is that upper layers are unaware of the reason why a packet was discarded at the physical layer. In general, a packet may be discarded due to two causes: a weak signal (due to attenuation and multipath characteristics of the environment) or interference due to concurrent transmissions from other neighboring devices. However, the MAC layer of IEEE 802.11 is unaware of the cause of the packet loss, resulting in loss of performance. The inability to detect collisions and distinguishing them from channel errors causes a waste of bandwidth (due to the colliding transmission), and an unnecessary delay due to performing a backoff. To address this issue, this paper introduces a mechanism to detect the cause of a packet loss in wireless networks using IEEE 802.11 as the MAC protocol.

Determining the actual cause of packet loss in wireless networks helps the MAC layer in making intelligent decisions. If a packet loss occurred due to a collision, an exponential backoff should be performed. Whereas, if a packet loss was the result of channel errors then a data rate adaptation algorithm should be invoked - possibly reducing the data rate and/or increasing the transmit power. It has been shown in [1] that knowledge of the cause of a packet loss can increase the throughput by 20-60% while reducing the retransmissions by 40%, depending upon the channel conditions. From the above discussion it is clear that the cause of a packet loss should be used by the MAC layer to improve performance in wireless networks.

A small number of techniques have been proposed in literature for collision detection in wireless networks. A mechanism for collision detection called CARA has been proposed in [3], and is based on the use of multiple RTS/CTS packets. RRAA [2] uses the CARA based RTS/CTS scheme to infer whether a packet loss is due to a collision or weak signal. A method to isolate physical packet errors from collision packet errors using RTS/CTS and packet fragmentation is given in [4]. These approaches require the observation and transmission of multiple RTS/CTS packets, thus requiring a long time to isolate the cause of a packet loss. In contrast, our approach to collision detection is more direct and is based on a metric that can be obtained immediately from the received packet, thus giving us immediate results in real time. In [1] a scheme for collision detection is proposed using three channel quality related metrics and a metric vote. Simulation results presented in this paper show that our proposed technique leads to significant reduction in the false positive rates and comparable detection accuracy.

A. Key Contributions

The following are the major contributions of this work.

1) Characterization of EVM in the presence of collisions: In this paper, we present an analytic model for the statistical behavior of EVM for the purpose of collision detection in wireless networks. Using a realistic model for wireless communication, we evaluate the probability distribution function (PDF) of EVM. This model is then used to derive analytical expressions that relate key parameters characterizing the cause of a packet loss to the statistical behavior of EVM.

2) Mechanism for Collision Detection: This paper proposes a mechanism to detect collisions using EVM. The collision

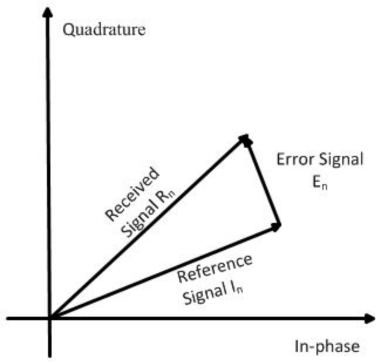

Fig. 1. Illustration of Error Vector

detection mechanism is based on using a threshold for the EVM to classify packets into collision or non-collision packets. To obtain the threshold, we first develop an analytic model to characterize the EVM in the presence and absence of collisions. The optimum EVM threshold for classification is then determined by deriving the threshold that leads to equal false positive and false negative rates. We evaluate the effectiveness of our collision detection mechanism by using extensive simulations.

The rest of this paper is organized as follows. Section II presents an analytic model for the EVM under different interference scenarios. The model for EVM is used in Section III to determine the threshold for classifying the cause of a packet loss. Finally, Section IV presents the details of the simulation model, Section V presents the simulation results and Section VI concludes the paper.

II. Analysis of EVM for Collision Detection

In this section we present a model to characterize the PDF of EVM in the presence and absence of collisions. This model is then used in the next section to develop a classifier for determining the cause of each packet loss.

An error vector is the difference between the complex voltage value of an ideal symbol and the actual received symbol. The root-mean-squared value of the error vector is defined as EVM. If X_k denotes the reference or transmitted signal and Y_k denotes the received (distorted) signal, then Figure 1 shows the error vector $E_k = Y_k - X_k$. Then the EVM is defined as [10]:

$$EVM_{RMS} = \sqrt{\frac{\frac{1}{N}\sum_{k=0}^{N-1}|Y_k - X_k|^2}{P_0}} = \sqrt{\frac{\frac{1}{N}\sum_{k=0}^{N-1}|E_k|^2}{P_0}} \quad (1)$$

where P_0 is the average power of all the symbols for a given modulation, and N is the number of received symbols. P_0 normalizes the EVM so that it does not depend on the modulation order.

A transmitted OFDM signal may experience various distortions during transmission, resulting in high values of EVM. The standards specify limits on the EVM to ensure satisfactory

TABLE I
Allowed EVM values versus data rate in IEEE 802.11

Data rate (Mbits/s)	EVM (dB)	EVM (%)
6	-5	56
9	-8	40
12	-10	32
18	-13	22
24	-16	16
36	-19	11
48	-22	8
54	-25	6

in-band performance [5]. The thresholds for EVM, as specified in the IEEE 802.11 standard [9], are given Table I.

Let us denote the transmitter by T_x, the receiver by R_x, and the interference by ζ_J (where J is the number of interferers). Let us consider an OFDM system with N subcarriers. We assume a frequency flat multipath Rayleigh fading channel. The received time domain OFDM signal y_n is given by

$$y_n = H_n * x_n + \eta_n + \zeta_n \quad (2)$$

where H_n denotes the Rayleigh distributed channel coefficients, η_n is the additive white Gaussian noise with zero-mean and variance σ_η^2, and ζ_n is the interference (due to a collision). x_n is the n^{th} time domain OFDM signal, $0 \le n \le N-1$. Then x_n can be obtained from X_k, the M-QAM modulated symbol at the k^{th} subcarrier as [7],

$$x_n = IDFT\{X_k\} = \sum_{k=0}^{N-1} X_k e^{j2\pi kn/N} \quad (3)$$

where $k = 0, 1, \cdots, N-1$. If the number of subcarriers N is large, the real and imaginary parts of x_n are approximately i.i.d. Gaussian distributed with zero-mean and variance σ_x^2 [5]. If we assume frequency flat fading, we can replace the convolution operator in Equation (2) with a multiplication and rewrite Equation (2), as

$$y_n = H_n x_n + \eta_n + \zeta_n. \quad (4)$$

Let us introduce a random variable Z defined as

$$Z = \frac{1}{N \cdot P_0}\sum_{k=0}^{N-1}|E_k|^2. \quad (5)$$

Let e_n denote the error vector in the time domain i.e., $e_n = y_n - x_n$. We also know that $e_n = \text{IDFT}\{E_k\}$ and $y_n = \text{IDFT}\{Y_k\}$. Therefore, applying Parseval's theorem, we can rewrite Equation (5) as

$$Z = \frac{1}{N \cdot P_0}\sum_{n=0}^{N-1}|e_n|^2. \quad (6)$$

Observing Equations (5) and (6), we see that Z is composed of the sum of N i.i.d. random variables. Applying the central limit theorem for large N (typically $N = 52$ for IEEE

802.11a), we can approximate Z by a Gaussian distribution with probability density function (PDF)

$$f_Z(z) = \frac{1}{\sqrt{2\pi\sigma_Z^2}} e^{-\frac{(z-\mu_z)^2}{2\sigma_Z^2}}. \tag{7}$$

To obtain the pdf $f_Z(z)$ of Z, we need to find its mean (μ_Z) and variance (σ_Z^2). μ_Z and σ_Z^2 will have different values for different types of distortions, and we are interested in finding them for packets involved in a collision. We first evaluate μ_Z and σ_Z^2 for the case when there is no collision. In this case the error vector is given by

$$e_n = H_n x_n + \eta_n - x_n = x_n(H_n - 1) + \eta_n. \tag{8}$$

We assume the standard path loss law $l(r) = \frac{1}{r_i^\alpha}$, and take $r_i^{-\alpha}$ as the mean power for a Rayleigh distributed channel (H_n). To find μ_Z, we have

$$\begin{aligned} \varepsilon\{Z\} = \mu_Z &= \frac{1}{N \cdot P_0} \sum_{n=0}^{N-1} \varepsilon\{|e_n|^2\} \\ &= \frac{1}{P_0}\left[\sigma_x^2\left(\frac{2}{r_i^\alpha} + 1 - 2\sqrt{\frac{\pi}{2r_i^\alpha}}\right) + \sigma_\eta^2\right] \end{aligned} \tag{13}$$

where $\varepsilon\{e_n^2\}$ is given by Equation (9). To find the variance of Z, we need to evaluate $\varepsilon\{Z^2\}$ given as follows:

$$Z^2 = \left(\frac{1}{NP_0}\sum_{n=0}^{N-1}|e_n|^2\right)^2 = \frac{1}{N^2P_0^2}\sum_{n_1=0}^{N-1}\sum_{n_2=0}^{N-1}|e_{n_1}|^2|e_{n_2}|^2. \tag{14}$$

We now assume block fading with a block length of m symbols. Then Equation (14) can be re-written as

$$\begin{aligned} Z^2 = \frac{1}{N^2P_0^2}&\Bigg[\left(\sum_{n_1=0}^{m-1}\sum_{n_2=0}^{m-1}|e_n|^4 + \sum_{n_1=0}^{m-1}\sum_{n_2=m}^{N-1}|e_{n_1}|^2|e_{n_2}|^2\right) + \\ &\left(\sum_{n_1=m}^{2m-1}\sum_{n_2=m}^{2m-1}|e_n|^4 + \sum_{n_1=m}^{2m-1}\sum_{n_2=0}^{m-1}|e_{n_1}|^2|e_{n_2}|^2 + \sum_{n_1=m}^{2m-1}\sum_{n_2=2m}^{N-1}|e_{n_1}|^2|e_{n_2}|^2\right) \\ &+ \cdots + \left(\sum_{n_1=\beta}^{N-1}\sum_{n_2=\beta}^{N-1}|e_n|^4 + \sum_{n_1=\beta}^{N-1}\sum_{n_2=0}^{\beta-1}|e_{n_1}|^2|e_{n_2}|^2\right)\Bigg]. \end{aligned} \tag{15}$$

where $\beta = N - m$. Taking the expectation of Equation (15), we get

$$\varepsilon\{Z^2\} = \frac{1}{NP_0^2}\left[m\varepsilon\{e_n^4\} + (N-m)\left(\varepsilon\{e_n^2\}\right)^2\right] \tag{16}$$

where $\varepsilon\{e_n^2\}$ and $\varepsilon\{e_n^4\}$ are given by Equations (9) and (10), respectively. Combining Equations (13) and (16), we can obtain the variance of Z as $\sigma_Z^2 = \varepsilon\{Z^2\} - (\mu_Z)^2$.

Now consider the case when a packet is corrupted due to the interference caused by collision from other concurrent transmissions. We assume a wireless network with J interferers at distance $r_j > 0$ from R_x, that transmit with a probability p independent of each other. We assume that the starting location of a collision within a packet is uniformly distributed between 0 and $N-1$. If a collision starts at OFDM symbol n_0, the error vector can be written as

$$e_n^* = \begin{cases} e_n & n < n_0 \\ e_n + \zeta_J & n \geq n_0 \end{cases} \tag{17}$$

where ζ_J is given as follows

$$\zeta_J = \sum_{i=0}^{J} B_i H_{r_i} W_i. \tag{18}$$

Here B_i's are i.i.d. Bernoulli random variables with parameter p, H_{r_i} is Rayleigh distributed with mean power $1/r_i^\alpha$, and W_i is the OFDM symbol transmitted by interferer i, which is approximately i.i.d. Gaussian distributed with zero-mean and variance σ_x^2. We can then rewrite Equation (6) as follows:

$$Z^* = \frac{1}{NP_0}\left(\sum_{n=0}^{n_0-1}|e_n|^2 + \sum_{n=n_0}^{N-1}(|e_n + \zeta_J|)^2\right). \tag{19}$$

Taking the expectation of Equation (19), we get

$$\begin{aligned} \varepsilon\{Z^*\} = \mu_{Z^*} = &\frac{1}{P_0}\left(\sigma_x^2\left\{\frac{2}{r_i^\alpha} + 1 - 2\sqrt{\frac{\pi}{2r_i^\alpha}}\right\} + \sigma_\eta^2\right) \\ &+ \left(\frac{N+1}{2N}\right)\frac{1}{P_0}\left(2p\sigma_x^2\sum_{j=0}^{J-1}\frac{1}{r_j^\alpha}\right). \end{aligned} \tag{20}$$

Similarly, to get the variance of Z^*, we need to evaluate $\varepsilon\{Z^{*2}\}$, which is given by

$$\begin{aligned} Z^{*2} &= \frac{1}{N^2P_0^2}\sum_{n_1=0}^{N-1}\sum_{n_2=0}^{N-1}|e_{n_1}^{*\,2}||e_{n_2}^{*\,2}| \\ &= \frac{1}{N^2P_0^2}\Bigg[\sum_{n_1=0}^{n_0-1}\sum_{n_2=0}^{n_0-1}|e_{n_1}^2||e_{n_2}^2| + \sum_{n_1=0}^{n_0-1}\sum_{n_2=n_0}^{N-1}|e_{n_1}^2||e_{n_2}^{*\,2}| + \\ &\quad\sum_{n_1=n_0}^{N-1}\sum_{n_2=0}^{n_0-1}|e_{n_1}^{*\,2}||e_{n_2}^2| + \sum_{n_1=n_0}^{N-1}\sum_{n_2=n_0}^{N-1}|e_{n_1}^{*\,2}||e_{n_2}^{*\,2}|\Bigg]. \end{aligned} \tag{21}$$

Taking the expectation of Equation (21), we get

$$\begin{aligned} \varepsilon\{Z^{*2}\} = \frac{1}{N^2P_0^2}&\Big[n_0.m\varepsilon\{e_n^4\} + n_0(n_0-m)\left(\varepsilon\{e_n^2\}\right)^2 + \\ &2n_0(N-n_0)\varepsilon\{e_n^2\}\varepsilon\{e_n^{*\,2}\} + m(N-n_0)\varepsilon\{e_n^{*\,4}\} + \\ &(N-n_0)(N-n_0-m)\left(\varepsilon\{e_n^{*\,2}\}\right)^2\Big]. \end{aligned} \tag{22}$$

Taking the expectation of Equation (23) w.r.t. n_0, we get

$$\begin{aligned} \varepsilon\{Z^{*2}\} = \frac{1}{N^2P_0^2}&\left[\frac{1}{2}m(N-1)\varepsilon\{e_n^4\} + \right. \\ &\left(\frac{1}{3}(N-1)^2 - \frac{1}{2}m(N-1)\right)\left(\varepsilon\{e_n^2\}\right)^2 + \\ &\left((N-1)\left(\frac{N+2}{3}\right)\right)\varepsilon\{e_n^2\}\varepsilon\{e_n^{*\,2}\} + \frac{1}{2}m(N+1)\varepsilon\{e_n^{*\,4}\} + \\ &\left.\left(\frac{1}{3}(N^2+N+1) - \frac{1}{2}m(N+1)\right)\left(\varepsilon\{e_n^{*\,2}\}\right)^2\right]. \end{aligned} \tag{23}$$

$$\varepsilon\{e_n^2\} = \sigma_x^2 \left\{ \frac{2}{r_i^\alpha} + 1 - 2\sqrt{\frac{\pi}{2r_i^\alpha}} \right\} + \sigma_\eta^2 \tag{9}$$

$$\varepsilon\{e_n^4\} = (3\sigma_x^4)\left(\frac{8}{r_i^{2\alpha}} - \frac{4}{r_i^{\frac{3}{2}\alpha}} + \frac{12}{r_i^\alpha} - 2\sqrt{\frac{2\pi}{r_i^\alpha}} + 1 \right) + 3\sigma_\eta^2 + 6\sigma_x^2\sigma_\eta^2 \left(\frac{2}{r_i^\alpha} - \sqrt{\frac{2\pi}{r_i^\alpha}} + 1 \right) \tag{10}$$

$$\varepsilon\{e_n^{*2}\} = \sigma_x^2 \left\{ \frac{2}{r_i^\alpha} + 1 - 2\sqrt{\frac{\pi}{2r_i^\alpha}} \right\} + \sigma_\eta^2 + 2p\sigma_x^2 \sum_{j=0}^{J} \frac{1}{r_j^\alpha} \tag{11}$$

$$\begin{aligned} \varepsilon\{e_n^{*4}\} = & \left[(3\sigma_x^4)\left(\frac{8}{r_i^{2\alpha}} - \frac{4}{r_i^{\frac{3}{2}\alpha}} + \frac{12}{r_i^\alpha} - 2\sqrt{\frac{2\pi}{r_i^\alpha}} + 1 \right) + 3\sigma_\eta^2 + 6\sigma_x^2\sigma_\eta^2 \left(\frac{2}{r_i^\alpha} - \sqrt{\frac{2\pi}{r_i^\alpha}} + 1 \right) \right] + \\ & 6\left[\sigma_x^2 \left\{ \frac{2}{r_i^\alpha} + 1 - 2\sqrt{\frac{\pi}{2r_i^\alpha}} \right\} + \sigma_\eta^2 \right] \left[2p\sigma_x^2 \sum_{j=0}^{J} \frac{1}{r_j^\alpha} \right] + 6p\sigma_x^4 \sum_{j=0}^{J} \frac{1}{r_j^{2\alpha}} \end{aligned} \tag{12}$$

where $\varepsilon\{e_n^2\}$ and $\varepsilon\{e_n^4\}$ are given by Equations (9) and (10), respectively, while $\varepsilon\{e_n^{*2}\}$ and $\varepsilon\{e_n^{*2}\}$ are given by Equations (11) and (12), respectively. Thus, we can now obtain the variance of Z^* as $\sigma_{Z^*}^2 = \varepsilon\{Z^{*2}\} - (\mu_{Z^*})^2$.

III. Threshold Based Collision Detection

In this section we describe our threshold based mechanism for collision detection and present the methodology for obtaining the threshold.

The proposed collision detection method is based on noting the difference in the pdf of EVM in the presence of a collision. To classify the cause of each packet loss, we first calculate the EVM of each received packet. This calculated EVM value is then compared against a threshold value. If the calculated EVM value is greater than the threshold, the packet is classified as a collision, and vice versa. The optimum value of the threshold is determined by choosing the threshold value that leads to equal false positive and false negative rates (i.e., the threshold that leads to the crossover error rate).

The probability of a false positive is defined as the probability that the cause of a packet loss is attributed to a collision, while the actual cause was a weak signal (not a collision). If we denote the threshold by γ, then the probability of a false positive is given by

$$P_Z[Z > \gamma] = P_e \left[1 - \int_{-\infty}^{\gamma} f_Z(z)\, dz \right] \tag{24}$$

where P_e is the symbol error rate for an M-QAM system. Similarly the probability of a false negative is defined as the probability that the cause of a packet loss is attributed to a weak signal, while the actual cause was a collision. The probability of a false negative can be expressed as follows:

$$P_{Z^*}[Z^* \leq \gamma] = P_e \left[\int_{-\infty}^{\gamma} f_{Z^*}(z^*)\, dz \right]. \tag{25}$$

To obtain the threshold that leads to the crossover error rate, we can find γ by equating Equations (24) and (25). Thus, to get the threshold we need to solve the following equation numerically:

$$\int_{-\infty}^{\gamma} f_Z(z)\, dz + \int_{-\infty}^{\gamma} f_{Z^*}(z^*)\, dz = 1. \tag{26}$$

Using the parameter values given in Table II, the numerical solutions for the threshold γ (absolute value and in dB scale) for 12Mbps (QPSK), 24Mbps (16QAM), and 48Mbps (64QAM) are given in Table III.

TABLE II
Parameters for finding the Threshold

Parameter	Value
P_0	2(QPSK), 10(16QAM), 42(64QAM)
σ_x^2	0.5
σ_η^2	1
r_i (meters)	3
r_j (meters)	3, 10, 15, 20, 30
α	2
N	32
m	16

TABLE III
Thresholds for Detecting Collisions

Modulation Type	Threshold for Z	Threshold (dB)
QPSK (12Mbps)	0.5977	-2.234
16QAM (24Mbps)	0.1197	-9.219
64QAM (48Mbps)	0.0286	-15.436

IV. Simulation Model

In this section we describe the simulation model used to evaluate the proposed collision detection mechanism. The simulator was created in MATLAB/Simulink. The transmitter and receiver models were designed according to the IEEE 802.11a specifications [9]. The wireless nodes in the simulation are connected through a frequency flat multipath Rayleigh fading channel. The channel is realized through the Jake's model [8]. OFDM is used at the physical layer. The modulation related

TABLE IV
MODULATION PARAMETERS

Data rate (Mbits/s)	Modulation	Coding rate (R)	Coded bits per sub-carrier (N_{BPSC})	Coded bits per OFDM symbol (N_{CBPS})	Data bits per OFDM symbol (N_{DBPS})
6	BPSK	1/2	1	48	24
9	BPSK	3/4	1	48	36
12	QPSK	1/2	2	96	48
18	QPSK	3/4	2	96	72
24	16QAM	1/2	4	192	96
36	16QAM	3/4	4	192	144
48	64QAM	2/3	6	288	192
54	64QAM	3/4	6	288	216

TABLE V
TIMING RELATED PARAMETERS

Parameter	Value
N_{SYM}: Samples per OFDM symbol	80
N_{FFT}: FFT Length	64
N_{SD}: Number of data subcarriers	48
N_{SP}: Number of pilot subcarriers	4
N_{ST}: Number of total subcarriers	52 ($N_{SD} + N_{SP}$)
N_{TRAIN}: Number of training symbols	2
Δ_F: Subcarrier frequency spacing	0.3125 MHz (=20 MHz/64)
T_{FFT}: IFFT/FFT period	3.2μs(1/Δ_F)
$T_{PREAMBLE}$: Preamble duration	8μs
T_{GI}: Guard Interval (GI) duration	0.8μs (T_{FFT}/4)
T_{GI2}: Training symbol GI duration	8μs
T_{SYM}: Symbol interval	4μs ($T_{GI} + T_{FFT}$)
T_{LONG}: Training sequence duration	8μs ($T_{GI2} + 2xT_{FFT}$)

parameters are given in Table IV, while the OFDM timing related parameters are given in Table V.

The network topology used in our simulations is shown in Figure 2. We have two transmitters (T_1 and T_2) and one receiver (R) in our network. T_2 acts as the interferer and introduces collisions into the network. The frame size for T_1 is fixed at 32 OFDM symbols, while the frame size of T_2 is uniformly distributed between 1 and 32 OFDM symbols. By varying the frame size of the interferer (T_2) we can simulate collisions occurring between packets of different size. The simulator also allows us to change the probability of collision in the network, giving us flexibility in terms of controlling our experiment.

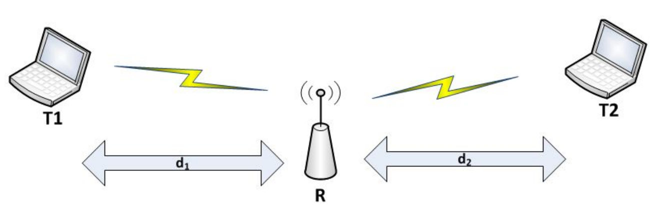

Fig. 2. Scenario for introducing collisions

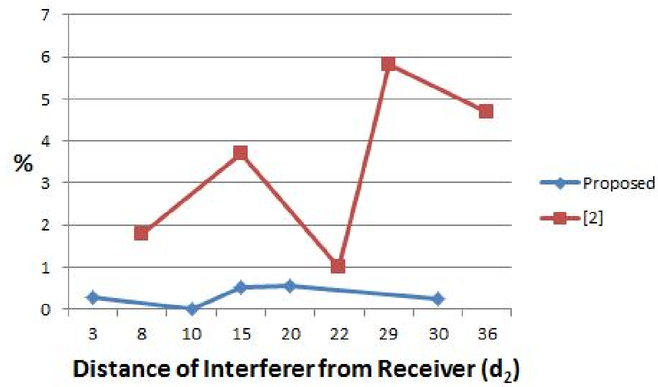

Fig. 3. Comparison of False Positive Rates

To model high mobility usage scenarios, the wireless channel assumes a maximum Doppler frequency of 100Hz. A high Doppler frequency also increases the probability of packet loss due to a weak signal. From the discussion in Section II it is clear that EVM does not depend on the modulation order, therefore we do not need to consider all the possible data rates. We simulate data rates of 12Mbps (QPSK), 24Mbps (16QAM), and 48Mbps (64QAM).

V. RESULTS

In this section we present simulation results to evaluate the performance of the proposed collision detection mechanism. We also compare the performance of the proposed mechanism with the most accurate detection mechanism in existing literature: a scheme proposed in [1] that uses three metrics, received signal strength, bit error rate and errors per symbol, to classify packets. The mechanism proposed in [1] uses a metric vote, i.e., whenever at least one of the metrics indicates a collision, the cause of packet loss is classified as a collision.

The performance of the proposed detection mechanism is evaluated in terms of two metrics: the false positive rate (defined as the proportion of the number of channel losses that were classified as collision losses) and the accuracy (defined as the proportion of the total number of classifications that were correct). The simulation settings used for obtaining the results are given in Section IV.

Figure 3 compares the false positive rates of the proposed mechanism and the mechanism from [1] as a function of the distance between the interferer and the receiver. We observe that the proposed mechanism has very low false positive rates and outperforms the classifier proposed in [1]. The corresponding accuracies for the two schemes is shown in Figure 4. We observe that while the scheme from [1] has better accuracy when the distance between the receiver and the interferer is small, our method performs better as this distance increases. However, it is important to note that the accuracy of the mechanism in [1] depends on the training data that is used to set its thresholds. In the simulation results reported here, the training and evaluation scenarios were quite similar, and the high accuracy is not surprising. In contrast, our mechanism

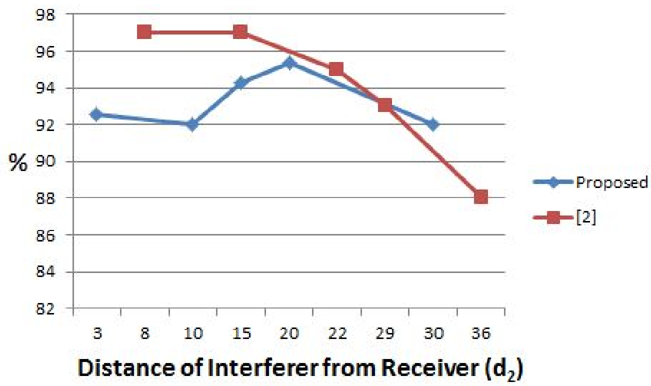

Fig. 4. Comparison of Accuracy

does not depend on any training data and is thus expected to be more robust in a variety of environments. In addition, the mechanism in [1] needs three metrics and thus has a higher complexity and overhead. The proposed scheme, however, is based on only one metric.

Overall, the proposed mechanism outperforms the mechanism in [1] in terms of the false positive rates and has comparable performance in terms of the accuracy, and this performance is achieved at lower complexity and greater robustness. Finally we note that another metric for comparing the performance of the classifiers is the false negative rate, defined as the proportion of collisions that were incorrectly classified as channel errors. Compared to the false negatives, the false positives have a more significant effect on the performance of a collision detection mechanism. A higher false positive rate will result in an increase in the number of backoffs and retransmissions. Thus it is desirable to keep the false positive rate as low as possible and the results show that the proposed mechanism is better at achieving this objective, as compared to the mechanism in [1].

VI. Conclusions

This paper proposed a mechanism based on EVM to determine the root cause of a packet loss in a wireless link. The proposed methodology is based on evaluating the EVM value associated with a packet and comparing it against a threshold value. An analytic model is proposed to determine the threshold value such that the crossover error rate is achieved. The proposed mechanism is compatible with existing OFDM based IEEE 802.11 hardware and protocol specifications. The accuracy of the proposed mechanism was evaluated and established through extensive simulation results.

References

[1] S. Rayanchu, A. Mishra, D. Agrawal, S. Saha, S. Benerjee, "Diagnosing Wireless Packet Losses in 802.11: Separating Collision from Weak Signal," *Proc. IEEE INFOCOM,* Phoenix, AZ, April 2008.

[2] S. H. Wong, H. Yang, L. Lu, and B. Bhargavan, "Robust Rate Adaptation in 802.11 Wireless Networks," *Proc. ACM MOBICOM,* Los Angeles, CA, September 2006.

[3] J. Kim, S. Kim, S. Choi, and D. Qiao, "CARA: Collision-aware rate adaptation for 802.11 WLANs," *Proc. IEEE INFOCOM,* Barcelona, Spain, March 2006.

[4] M. A. Y. Khan, and D. Veitch, "Isolating Physical PER for Smart Rate Selection in 802.11," *Proc. IEEE INFOCOM,* Rio de Jeneiro, Brazil, April 2009.

[5] C. Zhao, and R.J. Baxley, "Error Vector Magnitude Analysis for OFDM Systems," *Signals, Systems and Computers, 2006. ACSSC '06. Fortieth Asilomar Conference on ,* October 2006.

[6] L. L. Peterson, and B. S. Davie, "Computer Networks - A systems Approach," Elsevier Inc., 2007.

[7] Y. S. Choo, J. Kim, W. Y. Yang, and C. G. Kang, "MIMO-OFDM Wireless Communications with MATLAB," IEEE press, 2010.

[8] W. C. Jakes, "Microwave Mobile Communications," IEEE press, 1974.

[9] IEEE Standard 802.11a-1999, "High-speed Physical Layer in the 5 GHz Band," 1999.

[10] S. Forestier, P. Bouysse, R. Quere, A. Mallet, J. M. Nebus, and L. Lapierre, "Joint Optimization of the Power-Added Efficiency and the Error-Vector Measurement of 20-GHz pHEMT Amplifier through a New Dynamic Bias-Control Method," *IEEE Transactions on Microwave Theory Tech.,* vol.52, no.4, pp.1132-1141, 2004.